CALPHAD: Computer Coupling of Phase Diagrams and Thermochemistry 39 (2012) 97–103

Contents lists available at SciVerse ScienceDirect

CALPHAD: Computer Coupling of Phase Diagrams and Thermochemistry

journal homepage: www.elsevier.com/locate/calphad

First principles phase diagram calculations for the octahedral-interstitial system αTiO_X, $0 \le X \le 1/2$

Benjamin Paul Burton [a,*], Axel van de Walle [b]

[a] Materials Measurement Laboratory, Metallurgy Division, National Institute of Standards and Technology (NIST), Gaithersburg, MD 20899, USA
[b] School of Engineering, Brown University, Providence, RI 02912, USA

ARTICLE INFO

Article history:
Received 9 March 2012
Received in revised form
17 September 2012
Accepted 17 September 2012
Available online 16 October 2012

Keywords:
TiO_X
Ti suboxides
Devil's staircase
Long-period superstructures
First principles phase diagram calculation

ABSTRACT

First principles based phase diagram calculations were performed for the hexagonal closest packed octahedral-interstitial solid solution system αTiO_X, or $\alpha Ti[\ ]_{1-X}O_X$ ([ ]=Vacancy; $0 \le X \le 1/2$), by the cluster expansion (CE) method. The predicted diagram has ordered ground-state (GS) phases at: $X=0$ (hcp αTi, $P6_3mmc$); $X=1/6$ (Ti_6O: $P\bar{3}1c$, R3, $R\bar{3}$); $X \approx 1/3$ (Ti_3O: $R\bar{3}$, $P\bar{3}1c$, $R\bar{3}'$); and $X=1/2$ (Ti_2O: Pbcn; contrary to previous reports that it is anti-CdI_2). Both at $X=1/6$ and $X=1/3$ density functional theory (DFT) calculations predict at least triply degenerate GS (three structure energies at each composition that are within $\approx$ 0.001 eV; i.e. within DFT error). In the CE, this leads to exactly triply degenerate GS at both compositions. The calculated phase diagram includes a broad field between Ti_6O and Ti_3O in which the stable phases have layer-structures that are related to the anti-CdI_2-structure. It appears that disordering of the Ti_6O- and Ti_3O-GS involves cascades of first-order transitions that are suggestive of Devil's staircases.

Published by Elsevier Ltd.

1. Introduction

The group-IV hexagonal closest packed (hcp) suboxides αMO_X (M=Ti, Zr or Hf; $0 \le X \le 1/2$) all exhibit octahedral interstitial ordering of vacancies, [ ], and oxygen, O, ([ ] : O order–disorder) in solid solutions of the form $\alpha M[\ ]_{1-X}O_X$ ($0 \le X \le 1/2$). The most studied of these systems is αZrO_X, because of issues related to the oxidation of Zircaloy cladding on UO_2 fuel rods in light-water reactors [1–17]. The hcp-based αHfO_X alloys [18–22] are also potential cladding materials; e.g. for long-lived nuclear waste transmutation applications in boiling water reactors [23].

Hexagonal closest packed αTiO_X has received considerable attention as well, [5,6,24–36] presumably because of the importance of Ti-based light alloy materials, which necessitates a fundamental understanding of Ti-oxidation thermodynamics. Also, of course, investigating the chemical systematics of all three group-IV suboxides enhances understanding of each.

Long-period superstructure (LPSS) phases were reported in ZrO_X samples with with bulk compositions close to Zr_3O, [4,5,10] but first principles phase diagram (FPPD) calculations did not reproduce this [17]. Curiously however, FPPD calculations for HfO_X [18] predict cascades first-order transitions between closely related ordered structures at $X \approx 1/3$ and $X \approx 1/2$; and the FPPD calculations for TiO_X, described below, predict such cascades at $X \approx 1/6$ and $X \approx 1/3$. These predictions strongly suggest Devil's staircase [37,38] type disordering; i.e. infinite arrays of first-order transitions (singularities) between closely related structures.

2. Methodology

2.1. Total energy calculations

Formation energies, ΔE_f (Fig. 1) were calculated for fully relaxed hcp αTi, TiO (hcp αTi with all octahedral interstices occupied by O), and 96 $\alpha Ti_{m+n}[\ ]_mO_n$ supercells (m,n integers) of intermediate composition. All calculations were performed with the density functional theory (DFT) based Vienna *ab initio* simulati on program (VASP, version 4.4.5 [39,40]) using projector-augmented plane-wave pseudopotentials, and the generalized gradient approximation for exchange and correlation energies. Electronic degrees of freedom were optimized with a conjugate gradient algorithm, and both cell constant and ionic positions were fully relaxed.

Total energy calculations were converged with respect to k-point meshes by increasing the density of k-points for each structure until convergence was achieved. A 500 eV energy cutoff was used, in the "high precision" option which guarantees that *absolute* energies are converged to within a few meV/site (a few tenths of a kJ/site of exchangeable species; O, [ ]). Residual forces were typically 0.02 eV or less. An order of magnitude higher

* Corresponding author. Tel.: +1 301 975 6043.
E-mail address: benjamin.burton@nist.gov (B.P. Burton).

0364-5916/$ - see front matter Published by Elsevier Ltd.
http://dx.doi.org/10.1016/j.calphad.2012.09.004

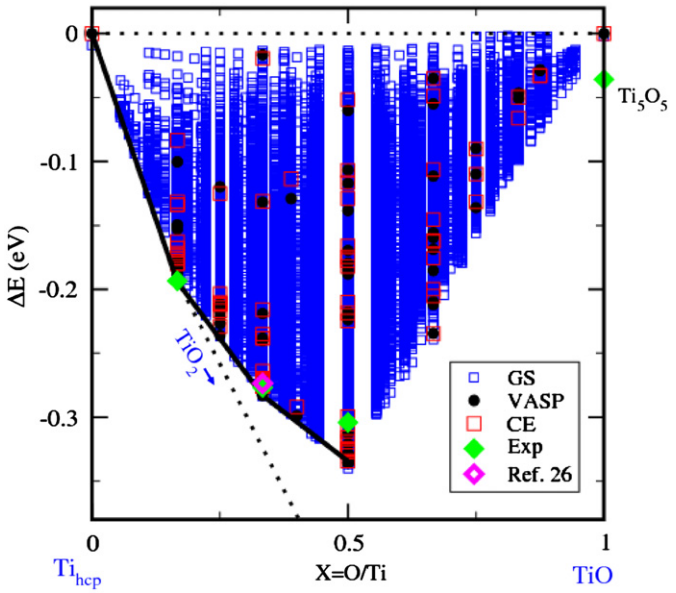

Fig. 1. Comparison of VASP (large solid circles) and CE (larger open squares, red online) formation energies, ΔE_f, and a ground-state analysis on structures with 18 or fewer octahedral-interstitial sites (smaller open squares, blue online). Extension of the convex hull towards the formation energy of rutile, TiO_2, indicates (contrary to experiment) that only the GS at $X=1/6$ is predicted to be stable. Solid diamonds (green online) indicate formation energies for experimentally determined structures: P$\bar{3}$1c structures at $X=1/6$ and $X=1/3$; [5,6,25,27,33] P $\bar{3}$ m1 at $X=1/2$ [33]; and C2/m Ti_5O_5 structure at $X=1.0$ [47–50]. The open diamond (magenta online) is the $X=1/3$ P312 symmetry structure proposed by Jostsons and Malin [26]. (For interpretation of the references to color in this figure caption, the reader is referred to the web version of this article.)

precision calculations were performed for the degenerate GS at $X=1/6$ and $X=1/3$.

Calculated formation energies, ΔE_f, relative to a mechanical mixture of αTi + αTiO, for the 96 $\alpha Ti_{m+n}[\ ]_m O_n$ supercells are plotted as solid circles in Fig. 1. Values of ΔE_f are

$$\Delta E_f = (E_{Str} - mE_{\alpha Ti} - nE_{\alpha TiO})/(m+n) \quad (1)$$

where E_{Str} is the total energy of the $\alpha Ti_{m+n}[\ ]_m O_n$ supercell, $E_{\alpha Ti}$ is the energy/atom of αTi, and $E_{\alpha TiO}$ is the energy/atom of αTiO.

2.2. The cluster expansion Hamiltonian

The cluster expansion (CE) technique [41], as described in [17] was used to model finite temperature order–disorder transitions. Fitting of the CE Hamiltonian and finite temperature simulations were performed with the alloy theoretic automated toolkit (ATAT) [40,42–44]. A complete description of the code's algorithms can be found in Ref. [43].

The zero- and point-cluster values were −0.341951 eV and −0.091967 eV, respectively. The seven pair, nine 3-body, and eleven 4-body effective cluster interactions (ECI) that comprise the CE-Hamiltonian are plotted in Fig. 2a and b (open symbols, blue online), as are ECI for αZrO_X (solid black symbols), and αHfO_X (open symbols, red online). As in αZrO_X and αHfO_X, nearest neighbor (nn) $O-O$ pairs are highly energetic, and therefore strongly avoided; hence nn-pair ECI are strongly *attractive* (ECI > 0, for *O*-[ ] nn pairs); but beyond nn-pairs, the pairwise ECI approach zero; however the 3′rd and 4′th nn pair-ECI in αHfO_X are significantly larger than corresponding terms for αZrO_X; while the 3'rd nn term for αTiO_X approaches zero, but the 4'th nn term for αTiO_X is comparable to that for αHfO_X. In αZrO_X and αHfO_X, the ratio of ECI parallel ($J_\parallel$) and perpendicular ($J_\perp$) to c_{Hex}, respectively, is $J_\parallel/J_\perp \approx 2.5$; but for αTiO_X, $J_\parallel/J_\perp \approx 5$. These results are similar to those in Ruban et al. [45], although the pairwise ECI reported here are not identically comparable owing to different treatments of relaxation energies, and Ruban et al. [45] ignore 3- and 4-body terms. The relatively large (negative) three-body terms in the αZrO_X and αTiO_X ECI-sets are both for linear triplet interactions parallel to c_{Hex}. These ECI reflect the energetic favorability of layer-structures in which O-rich and O-poor layers, that are perpendicular to c_{Hex}, alternate along c_{Hex}.

3. Results

3.1. Ground-states and their order–disorder transitions

The CE was used for a ground-state (GS) analysis that included all configurations of [ ] and *O* in systems of 18 or fewer *Ti*-atoms (octahedral interstitial sites); a total of $2^{18} = 262{,}144$ structures. Four GS were identified in the range, $0 \le X \le 1/2$, i.e. at $X=0$, 1/6, 1/3, and 1/2; solid circles (black online) on the convex hull (solid line) in Fig. 1. Larger open squares (red online) in Fig. 1 are CE-calculated values for the ΔE_f that correspond to the VASP calculations, and the smaller open squares (blue online) are ΔE_f for the remaining 262,144-83=262,061 structures in the GS analysis. All space group determinations were performed with the FINDSYM program [40,46].

The extension of the convex hull towards rutile-structure (TiO_2) is plotted in Fig. 1, and contrary to experiment, it suggests that Ti_6O is the only stable low-T sub-oxide phase. A low-temperature TiO phase has been reported (monoclinic C2/m Ti_5O_5 [47–50]) but its calculated formation energy is only 0.036 eV lower than that of the hcp-based TiO compound, which is 0.285 eV below the NaCl-structure phase (not shown). Experiment suggests that a low-temperature TiO-phase, is stable, in equilibrium with a solid solution of bulk composition $X \lesssim 0.42$, [35,36], thus it seems likely that some TiO-composition phase has much lower energy than Ti_5O_5. The observed Ti_5O_5-phase may be a quenched higher-T state, and/or the PAW-GGA formation energy for rutile-structure (TiO_2) may be significantly more negative than it should be. Idealized GS structures at $X=1/6$, $X=1/3$ and $X=1/2$ are shown in Fig. 3.

3.2. Ti_6O

3.2.1. The Ti_6O ground-state

Kornilov [33] (also [25,27]) reported the low-T Ti_6O space group symmetry as P$\bar{3}$1c (solid diamond, Fig. 1, green online). VASP calculations yield three Ti_6O formation energies within ≈0.001 eV of one another, i.e. within DFT error. The triply degenerate GS at $X=1/6$ includes a R$\bar{3}$ structure, the P$\bar{3}$1c structure, and a R3 (Fig. 1); their O:[ ] configurations are shown in Fig. 4. All three of these structures consist of $[\ ]_{2/3}$:$O_{1/3}$-mixed-layers that alternate with [ ]-layers perpendicular to c_{Hex}. Differences in the formation energies for these structures depend on interactions across two or more atomic layers, and these interactions are evidently vanishingly small in the VASP results (and presumably in the real system), and they are exactly zero in the CE. It also implies an infinity of degenerate GS based, at least, on different stacking sequences of the three identified degenerate GS, perpendicular to c_{Hex}.

3.2.2. Order–disorder in Ti_6O

As shown in Fig. 5a–d the Ti_6O-GS is predicted to disorder via a staircase of first-order transitions, both as functions of T (Fig. 5a,c,d) and X (Fig. 5b). Here the order parameter is defined as the sum of fractional occupancies of sites in the GS-starting-configuration that retain GS-occupations, normalized to the number of sites. As a function of X, the expected two-phase fields, between adjoining stair-step phases, are vanishingly narrow, owing to the vanishingly small free-energy differences between them. Also, the predicted onsets of staircase disordering do not follow simple monotonic trends: (1) using different (degenerate) GS as MC-starting configurations yields different onsets, (2) different MC-simulation T-steps yield different onsets (online T-step=1 K, 0.5 K, 0.1 K correspond to black, blue, red triangles, respectively), and (3) even when GS-configuration and T-step are the same onsets may vary, owing to different random numbers in different MC-simulations. Disordering of the $O_{1/3}[\ ]_{2/3}$-mixed-layers yields the anti-CdI_2 structure (α'-phase) and disordering of the α'-layer-structure yields the disordered αTiO_X solid solution (α-phase). Thus, the high-T limit of the staircase is the α' anti-CdI_2 structure phase.

3.3. Ti_3O

3.3.1. The Ti_3O ground state

Yamaguchi [27] reported a low-T Ti_3O structure with P$\bar{3}$1c space group symmetry (solid diamond, Fig. 1, green online). This structure is among the three